Water Flow Based Complex Feature Extraction

Xin U Liu, Mark S Nixon

ISIS group, School of ECS, University of Southampton, Southampton, SO17 1BJ, U.K.
{xl104r, M.S.Nixon}@ecs.soton.ac.uk

Abstract. A new general framework for shape extraction is presented, based on the paradigm of water flow. The mechanism embodies the fluidity of water and hence can detect complex shapes. A new snake-like force functional combining edge-based and region-based forces produces capability for both range and accuracy. Properties analogous to surface tension and adhesion are also applied so that the smoothness of the evolving contour and the ability to flow into narrow branches can be controlled. The method has been assessed on synthetic and natural images, and shows encouraging detection performance and ability to handle noise, consistent with properties included in its formulation.

1. Introduction

Complex shape extraction is of great interest in practical uses such as vessel detection in iridology. There are two popular techniques which both involve contour evolution: active contours or snakes, and region growing.

Snakes evolve a parameterized curve from an initial position to the boundaries of the object following some rules to minimize a specified energy functional. The functional is defined so that the minimization can give rise to a smooth and even contour. In complex feature extraction, however, the classical snake is of limited use as it needs good initialization near the boundary and cannot handle topological changes like boundary concavities. Many methods have been proposed to overcome these problems. The balloon models [1], distance potentials [2], and gradient vector flow (GVR) field [3] have been introduced as the solutions of initialization and concave boundary detection. Snake energy functionals using region statistics or likelihood information have also been proposed [4, 5]. A common premise is to increase the capture range of the external forces to guide the curve towards the boundaries. For more complex topology detection, several authors have proposed adaptive methods like the T-snake [6] based on repeated sampling of the evolving contour on an affine grid. Geometric active contours [7,8] have also been developed where the planar curve is represented as a level set of an appropriate 2-D surface. They work on a fixed grid and can automatically handle topological changes. However, many methods solve only one problem whilst introducing new difficulties. The balloon models introduce an inflation force so that it can “pull” or “push” the curve to the target boundary, but the force cannot be too strong otherwise “weak” edges would be overwhelmed. Region-based energy can give a large basin of attraction and can converge even when the explicit edges do not exist but it cannot yield as good localization of the contour

near the boundaries as edge-based methods. Level set methods detect complex shapes well at the cost of increased dimensionality and hence much greater complexity.

The region growing techniques mainly rely on the assumption that adjacent pixels in the same object or region have similar characteristics such as intensity and texture. They test the statistics inside the growing region and then decide whether or not the adjacent pixel can be merged according to the specified homogeneity criterion. Region growing techniques are free of topological changes since they are pixel-wise techniques without smoothness constraints [9]. However, this property also tends to yield irregular boundaries and small holes, especially for noisy images [10]. Besides, the region statistics comparison standards on which they are based can lead to inaccurate contour detection.

This paper proposes a new feature extraction method based on water flow. Unlike the famous watershed method, which is based on mathematical morphology and is often combined with snakes [11] and region growing [12], the focus is now on the "water" itself rather than the "landscape" of images because the properties of water, like fluidity and surface tension, are well suited to complex feature extraction. We first introduce the related physical principles and the framework of the technique, and then define all the analogical factors. Finally, results both for synthetic and for real iris images are presented, which show the resolution of problems like topological changes, and good noise immunity.

2. Methodology

Water flow is a compromise between several factors: the position of the leading front of a water flow depends on pressure, surface tension, adhesion/capillarity. There are some other natural properties like turbulence and viscosity, which are ignored here. Image edges and some other characteristics that can be used to distinguish objects are treated as the "walls" terminating the flow. The final static shape of the water should describe the related object's contour.

The flow is determined by pressure and the resistance. The relationship between the flow rate f_r, the flow resistance R and the pressure difference, is given by:

$$f_r = Pi - Po \tag{1}$$

where P_i and P_o are pressure of the inflow and outflow, respectively. The pressure difference drives the flow and

$$f_r = AV_{effective} \tag{2}$$

where A is the cross-sectional area and $V_{effective}$ is the effective flow velocity. Hence the velocity can be related to force and resistance through equations (1) and (2).

There are small discontinuities or weak regions existent on the contours which may lead to "leakage" of water. The surface tension, which can form a water "film" to bridge gaps, is then applied to overcome the problem. An attractive force existing between water and walls, named adhesion is defined as the attractive force generated by image edges. It is adopted in the new technique to assist surface tension to bridge edge gaps and allow flow into narrow braches.

2.1 Framework of the Operator

The method has little dependence on the starting contour shape. The only limitation on initialization is that it cannot cross the target object's boundaries. One pixel in the image is considered to be one basic unit of the water, and the pressure between an element and each of its neighbors is assumed to be the same. An adaptive source is assumed so that the water can keep flowing until stasis, where flow ceases. An inner element with symmetrical distribution of neighbors hence suffers zero resultant pressure. A water contour element, however, has asymmetrically distributed neighbors (and possibly an additional adhesive force), thus has non-zero pressure difference which leads to a non-zero velocity by equations (1) and (2), and is possible to move outwards. Hence only boundary elements are of interest.

The flow process is assumed to be made up of two separable steps. The first stage is *acceleration*: the contour element achieves a velocity due to the presence of the pressure difference (and any adhesive force), and the ultimate value is given by equation (1) and (2). The next step is *external movement* where the moving element is now free from the influence from other water elements and suffers only external image forces. This is not consistent with a real action but is sufficient for the digital image analogy and greatly simplifies the algorithm.

The water element can move outwards in any direction for which the component of velocity is positive. However, only if the velocity in the direction is sufficiently large, can the element break through the image resistant forces and reach the new position. To reconcile the flow velocity with forces, dynamical formulae are used. We may compute the displacement of a contour element on each possible direction within a fixed time interval, which is similar to snake techniques. However, for simplicity and avoiding the interpolation problem, a framework like region growing and the greedy snake is used: the element will flow to some positions if certain conditions or formulae are satisfied. Here, an equation describing the *conservation of energy* is employed. If assuming that an element, which has a positive velocity v on a particular direction and is acted by the force F during the process, can arrive at the direction-related position ultimately, then this equalization must be fulfilled:

$$mv_F^2/2 = FS + mv^2/2 \quad (3)$$

where v_F is the final scalar velocity after fixed displacement S and m is the assumed mass. In this equation, force F is a scalar which is positive when the force is consistent with velocity v, and negative otherwise. The summation on the right hand side is just the movement decision operator: only if F is negative, can the summation be negative and thus the equality above cannot be satisfied.

2.2 Flow Driving Force with Surface Tension

The pressure on each contour element should be outwards normal to the contour line. Since the flow on each possible direction will be examined separately, the related component of forces rather than the composition is of interest, and a simple convolution method is used. The force on a contour element is determined by the surface interior i.e., the amount and position of the adjacent elements. For a certain direction, the-

Fig. 1. the convolution masks for component forces on the direction of (from left to right) 90 degrees, 0 degree, 135 degrees, and 45 degrees. The other 4 masks are the transpose of these and we can define the driving force on the opposite direction as negative.

re will be supporting and opposing elements. The property is determined by their relative position to the flow direction. The elements located at the normal to the direction do not affect the movement. The ones located at the inner half exhibit positive effects on the flow and the opposite ones give negative forces since the interactive force between elements is repulsion. The 3×3 templates are shown by figure 1. A matrix **W** is used to save the water information where a water element has value one and others are all zeros. Denoting the convolution template for direction i as $\mathbf{T}_i$, the corresponding matrix saving the normalized driving force strength on direction i, $\mathbf{F}_{D,,i}$, is then calculated by convolution as:

$$\mathbf{F}_{D,i} = \mathbf{W}*\mathbf{T}_i / S_{PM} \quad (4)$$

where S_{PM} is the possible maximum of the convolution sums. For each mask, the maximal value is achieved when water elements locate at all positions of 1's and none of those of -1's and hence $S_{PM} = 3$ for the above masks. The driving force strength on direction i at point (x, y) is then just the (x, y)th entry of $\mathbf{F}_{D,i}$.

The convolution mechanism allows situations of more than two adjacent contour elements which is common in complex shape extraction. The mask size can be expanded so that more information of local water structure can be involved and the calculation will be expected to give a more reasonable result. For instance, a single line would have smaller driving force when using 5*5 mask than that by a 3*3 one because the possible maximum is much larger but the convolution sum is just increased by 1. In addition, the method makes the application of surface tension more straightforward. From physics, the surface tension is decided by the temperature and the water itself. In this image analogy, it is defined as a constant *attractive* force between the contour elements. So in the previous convolution, we can just modify the water matrix with the contour position information so that the point will exhibit attractive forces. This is done by setting contour elements entries in **W** as fixed negative values, like -t. Then, replacing **W** in equation (5) with the new matrix **W'** and noting that the possible maximum is now (3+2t) will give the driving force combined with surface tension. Here, we set t=1.

2.3 Resistance to Flow and the Velocity

From equation (1) and (2), the flow velocity is inversely proportional to the resistance of water. In a physical model, the *flow resistance* is decided by the water, the flow channel and temperature etc. Since this is a physical analogy which offers great freedom in selection of parameter definitions, we can assign high resistance values for

unwanted image attributes and low values to preferred ones. For instance, in vessel detection in images of the retina, if the vessels have relatively low intensity, we can define the resistance to be proportional to the intensity of the pixel. If we couple the resistance with the edge information, the process will become adaptive. That is, when the edge response is strong, resistance would be large and so the flow velocity would be weakened. According to equation (3), the movement decision will now be dominated by the force acting during the exterior movement. Thereby, even if the driving force set by users is too "strong", the resistance would lower its influence at edge positions and the problem in balloon models [1], where strong driving forces may overwhelm "weak" edges, can be eliminated. From equations (1) and (2), the velocity is:

$$\mathbf{V}_i = \mathbf{F}_i / AR \tag{5}$$

where $\mathbf{V}_i$ is the resulting flow velocity. The direction of $\mathbf{V}$ is the same as the force $\mathbf{F}_i$. In this paper, A is set as a constant, and R at position (u, v) is determined by

$$R(u,v) = \exp\{-k\ \mathbf{E}(u,v)\} \tag{6}$$

where $\mathbf{E}$ is the edge response matrix and k controls the fall of the exponential curve.

2.4 Image Forces

The gradient of an edge response map is often defined as the potential force in active contour methods since it gives rise to vectors pointing to the edge lines [3]. This is also used here. The force is large only in the immediate vicinity of edges and always pointing towards them. The second property means that the forces at two sides of an edge have opposite directions. Thus it will attract water elements onto edges and prevent overflow. The potential force on a contour element (x_c, y_c) is given by:

$$\mathbf{F}_P = \bigtriangledown\mathbf{E}(x_t, y_t) \tag{7}$$

where $\bigtriangledown\mathbf{E}$ is the gradient of the edge map, and (x_t, y_t) are the coordinates of the flow target because the potential force is presumed to act during the second stage of flow where the element has left the contour and is moving to the target.

Adhesion is defined as the attraction between water and adjacent vessel walls in physics. In the image analogy, it is determined by potential force based on an edge map with "flooded" positions set to zero. In this map, the edges that have been occupied by the water are ignored so that the edges are clipped. As water flows, vectors (forces) pointing from the flooded edges to the existent ones are generated iteratively and thus assist in flow to the reserved edge lines. It is defined as

$$\mathbf{F}_A = \bigtriangledown\mathbf{D}(x, y) \tag{8}$$

where $\mathbf{D}$ is the edge map eroded by the flowing water and (x, y) are the coordinates of a contour point. This equation effectively defines the attractive force from edges to the water. Therefore, even if the water has flowed onto an edge point, it can still move to the adjacent edges. This will thus help water flow into narrow branches, and "flood" small noise pixel clusters to give noise robustness.

The forces defined above work well as long as the gradient of edges pointing to the boundary is correct and meaningful. However, as with corners, the gradient can

sometimes provide useless or even incorrect information. Unlike the method used in the inflation force [1] and T-snake [6], where the evolution is turned off when the intensity is bigger than some threshold, we propose a *pixel-wise* regional statistics based image force. The statistics of the region inside and outside the contour are considered respectively and thus yield a new image force:

$$F_S = -(\mathbf{I}(x_t, y_t) - \mu_{int})^2 \, n_{int}/(n_{int}+1) + (\mathbf{I}(x_t, y_t) - \mu_{ext})^2 \, n_{ext}/(n_{ext}+1) \quad (\mathbf{9})$$

where subscripts "*int*" and "*ext*" denote inner and outer parts of the water, respectively; μ and n are the mean intensity and number of pixels of each area, separately; **I** is the original image. The equation is deduced from the Mumford-Shah functional [5]:

$$F_1(C) + F_2(C) = \int_{inside(C)} |\mathbf{I}(x, y) - \mu_{int}|^2 + \int_{outside(C)} |\mathbf{I}(x, y) - \mu_{ext}|^2 \quad (\mathbf{10})$$

where C is the closed evolving curve. If we assume C_0 is the real boundary of the object in the image, then when C fits C_0, the term will achieve the minimum. Instead of globally minimizing the term as in [5], we obtain equation (9) by looking at the change of the total sum given by *single* movement of the water element. If an image pixel is flooded by water, the statistics of the two areas (water and non-water) will change and are given by equation (9). The derivation is shown in the Appendix.

The edge-based potential forces can provide a good localization of the contour near the real boundaries (i.e., accuracy) but have very limited capture range and are not suitable for edge corners, whilst the region-based forces have a large basin of attraction but cannot provide good detection accuracy. The complementary properties motivate a unification of the two forces. A convex combination method is hence chosen and the combined force is given by:

$$F = \alpha F_P + (1-\alpha) F_S \quad (\mathbf{11})$$

where all terms are scalar quantities, and α ($0 \le \alpha \le 1$) is determined by the user to control the balance between them.

2.5 Movement Decision Process

Equation (3) has provided the inequality to determine the feasibility of outwards flow. For each contour element, we have presented equations computing driving force $\mathbf{F}_\mathrm{D}$ modified by surface tension, adhesion $\mathbf{F}_\mathrm{A}$ and resistance R. Flow velocity **V** can then be obtained through equation (5). If the velocity points towards the exterior of the water, the element is assumed to leave the original position. A unified image force **F** provided by equations (7) and (11) is then turned on. The summation in equation (3) can be computed and the sign determines the result of the movement.

Defining m and S in equation (3) as constants, we can then present the new and detailed expression with parameters defined before:

$$J = \lambda \{ {}^{(FD+FA)}/_{R(x, y)} \}^2 + F \quad (\mathbf{12})$$

where λ is a regularization parameter set by users which controls the tradeoff between the two energy terms. It can be considered to be determined by the combination of mass m, displacement S and area A. Its value reflects smoothing of image noise. For example, more noise requires larger λ. F_A and F_D are the scalar components on the

movement direction of $\mathbf{F}_A$ and $\mathbf{F}_D$, respectively. A positive direction is defined from the origin to the target. The movement decision can be completely made by this operator since the term of right hand side inside the brackets gives the velocity information and J corresponds to the ultimate kinetic energy. If the velocity component is greater than zero and if J is positive, the movement is said to be feasible and the target point will be flooded by water.

3. Experimental Results

The new technique is applied to both synthetic and natural images, and is evaluated both qualitatively and quantitatively.

3.1 Synthetic Images

There are two sorts of initialization for the method. The water "source" can be either inside or outside the target object. The former is suited to most cases, whilst the latter is useful when simultaneously detecting multiple objects in an image. The whole "background" will be flooded, thus the static water will give the targets' shape information. An example is given in figure 2 with initialization from the image border. All the shapes are detected including the helical pipe which has boundary concavities. The result is accurate even with some noise contamination.

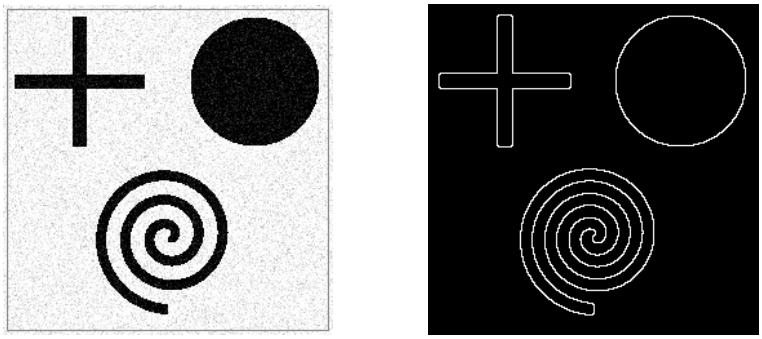

Fig. 2. Multi-object detection: the image is corrupted with 10% Gaussian noise

A 512×512 test image was generated for a performance evaluation according to certain criterion: a) horizontal, vertical and diagonal branches are included; b) narrow and wide branches are presented, respectively; c) there is a circular pipe so that we get a curve with smoothly changing curvature; d) each half of the object has a different intensity so that weak edges exist between them. The image is suited to assess the operator's ability in complex feature detection, and the noise immunity is also tested by adding Gaussian and impulsive noise to the image. Figure 3 shows the evolutions and the final results. The detection is successful in total, and the immunity to impulsive noise should be emphasized. It's very difficult for snakes and region growing methods

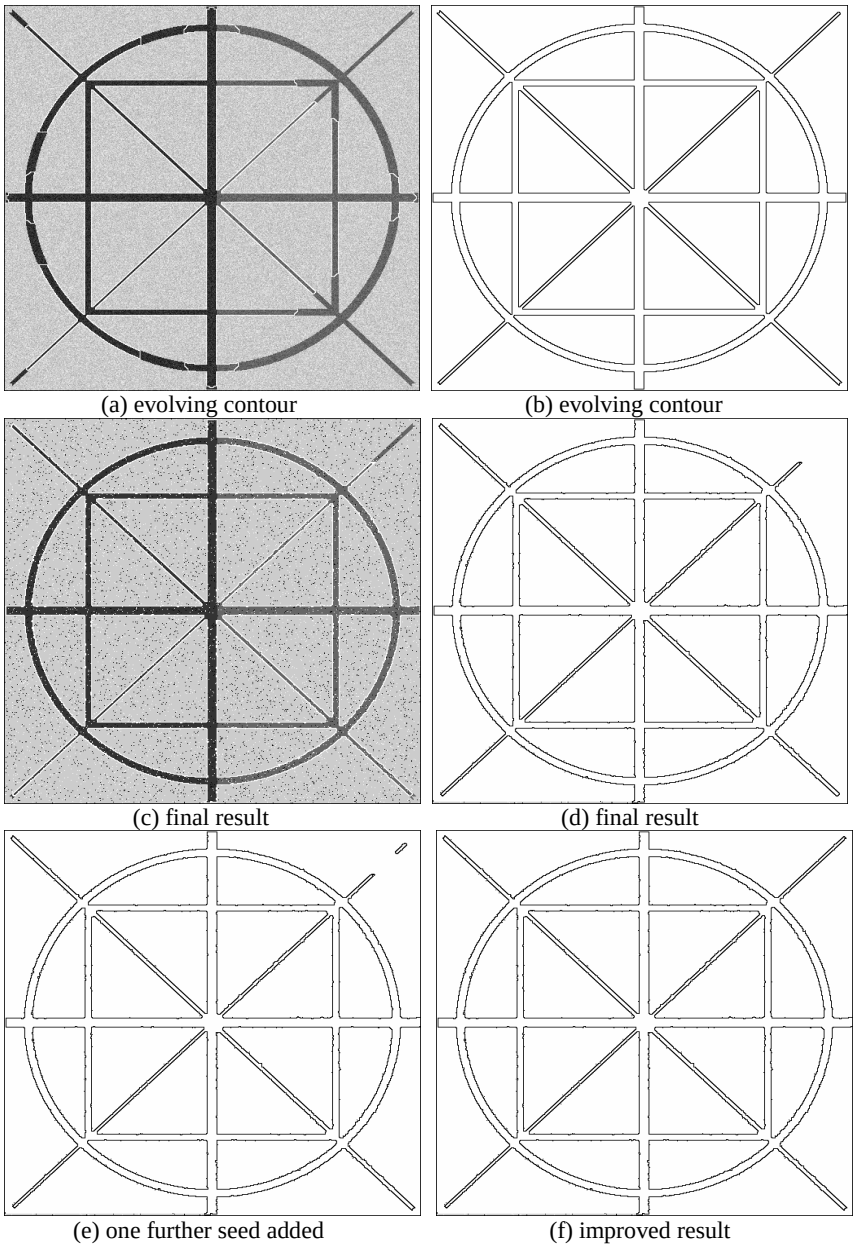

Fig. 3. Flow progress and results for test images contaminated by 10% Gaussian noise (a and b) and 5% impulsive noise (c, d, e and f).

to deal with impulsive noise as the edge response is very strong. In figure 3(c) and (d), almost all the noise points inside the object are flooded, and the detected contour is reasonably accurate. The robustness to impulsive noise arises from the fluidity and

the adhesion: water surrounds the small clusters of impulsive noise pixels, and the adhesive force given by the noise response attracts the water to flow over the noise area. So, unless the noise clusters are too large, the noise pixels will be flooded.

The most significant failure shown by figure 3(d) is the incomplete detection of the thinnest diagonal branch in the top right corner. This is because the branch is too narrow and a noise cluster "blocks" the pipe. In practical applications, this kind of gap will exist and makes the contour extraction terminate early. Flow from multiple sources can be considered, to overcome the problem. In this simple case, as shown in figures 3(e) and (f), a new source is initialized inside the undetected area. It then fills the region and merges with the "main" part. Therefore a complete detection can be achieved. Similar multiple seeds methods are often incorporated with watershed and region growing techniques, and are not invoked here.

The immunity to noise is also assessed quantitatively, and figure 4 shows the result. The mean square error is used as the criterion with a synthetic test image as the ground truth, which has been deliberately designed to incorporate a narrow boundary concavity. Two typical sorts of noise, Gaussian and impulsive, are added on the image, and the operator performs well and stably for both types of noise, until severe noise contamination (below 10 dB). An example of the detection result is also shown.

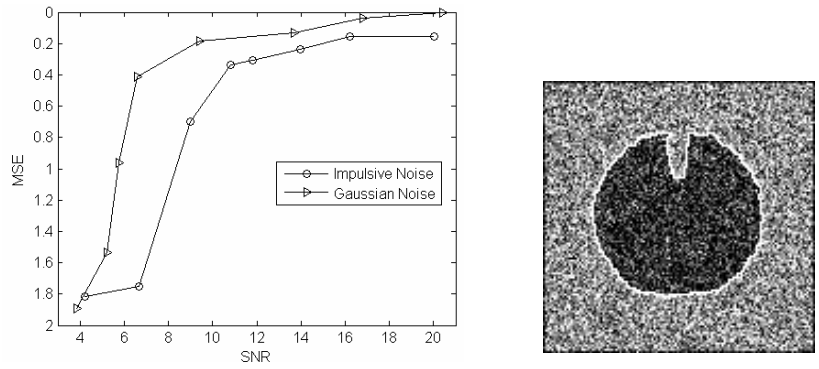

Fig. 4. Mean square error results for impulsive and Gaussian noise in different SNR levels. (α=0.5, $0.5 \leq \lambda \leq 1$, k=5); and an example for Gaussian noisy image (SNR=6.58, MSE=0.41). (note that the y-axis has been reversed for the conventional curve indication purpose).

3.2 Natural Images

Natural images with complex topology are also assessed. Figure 5 shows the result for the image of a river delta with different parameters, where the river is the target object. It is suited to performance evaluation since gaps and "weak" edges exist in the image. One example is the upper part of the river, where boundaries are blurred and irregular. There are also inhomogeneous areas inside the river, which are small islands and have lower intensity. Our water flow based operator can overcome these problems. As shown in figure 5 (a), a reasonably accurate and detailed contour of the river is extracted. At the upper area, some very weak boundaries are also detected. This is achieved by using high value of k which makes the operator highly sensitive to

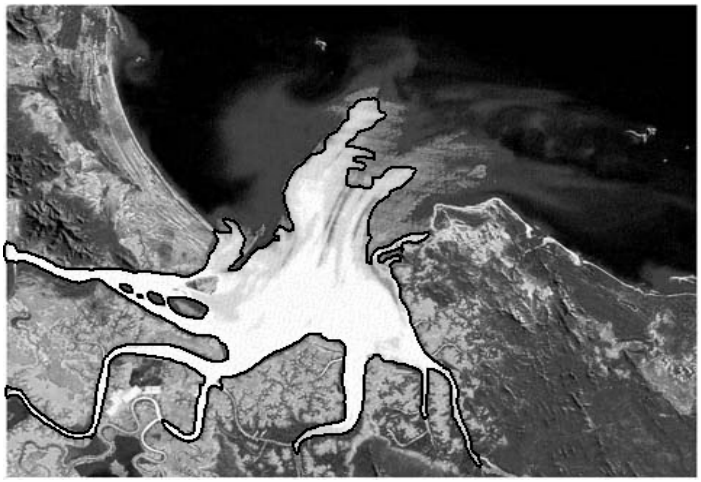

(a) α=0.7, λ=3, *k*=50

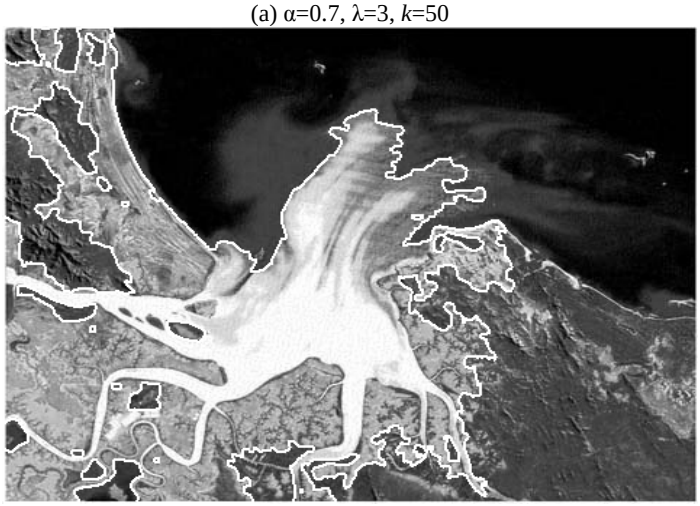

(b) α=0.5, λ=0.1, *k*=0

Fig. 5. water-flow detection results for delta map image with different parameters: decreased α and λ reduce the significance of edges, and smaller *k* makes flow less sensitive to edges, therefore the detail detection level is lower in (b).

edge response. The contour is relatively smooth by virtue of surface tension. The fluidity leading to topological adaptability is shown well by successful flow to the branches at the lower area. Most of them are detected except failure at several narrow branches. The barriers are caused either by natural irregularities inside them or noise.

Different initializations inside the river were tried and with the same parameters chosen, the results are almost the same, as expected. The operator is insensitive to the source positions. By changing the parameters, however, some alternative results can be achieved. For example, figure 5(b) shows a segmentation of the whole basin of the river. It is analogy to a flood from the river. The water floods the original channels

and stops at the relatively high regions. This shows the possibility of achieving different level of detail just by altering some parameters.

4. Conclusions

This paper introduces a new general feature extraction framework. The operator successfully implements the key attributes of water flow process: the fluidity, the surface tension and the adhesion. The resistance given by images is defined by a combination of object boundary and regional information. The problems of complex topological changes are solved whilst the attractive properties of snakes such as the smooth contour is retained. Those are approved by the results on both synthetic and real images. Good noise immunity is also justified both qualitatively and quantitatively. Besides, the complexity of the algorithm is relatively low. Therefore the method is expected to be of potential use in practical areas like medical imaging and remote sensing where target objects are often complicated shapes corrupted by noise.

References

[1] L. D. Cohen, "On active contour models and balloons," *CVGIP, Image Understanding*, 53(2): 211-218, 1991.

[2] L. D. Cohen and I. Cohen, "Finite element methods for active models and balloons for 2-D and 3-D images," *IEEE Trans. PAMI*, 15: 1131-1147, 1993.

[3] C. Xu and J. L. Prince, "Snakes, shapes, and gradient vector flow," *IEEE Trans. Image Processing*, 7(3): 359-369, 1998.

[4] M. Figueiredo and J. Leitao, "Bayesian estimation of ventricular contours in angiographic images," *IEEE Trans. Medical Imaging*, 11: 416-429, 1992.

[5] T. F. Chan and L. A. Vese, "Active contours without edges," *IEEE Trans. Image Processing*, 10: 266-276, 2001.

[6] T. McInerney and D. Terzopoulos, "Topologically adaptive snakes," *Int'l Conf. Computer Vision 95*, pp. 840-845, 1995.

[7] V. Casselles, R. Kimmel, and G. Spiro, "Geodesic active contours," *International Journal of Computer Vision*, 22(1):61-79, 1997.

[8] R. Malladi et al., "Shape modeling with front propagation: A level set approach," *IEEE Trans. PAMI*, 17: 158-174.

[9] R. Adams, and L. Bischof, "Seeded region growing," *IEEE Trans. PAMI*, 16(6): 641-647.

[10] S.C.Zhu and A.Yuille, "Region competition: unifying snakes, region growing, and Bayes/MDL for multi-band image segmentation," *IEEE Trans. PAMI*, 18(9): 884-900.

[11] V. Kiran, P. K. Bora, "Watersnake: integrating the watershed and the active contour algorithms," *TENCON 2003. Conference on Convergent Technologies for Asia-Pacific Region*, vol. 2, pp. 868-871, Oct. 2003

[12] A. Bleau and L. J. Leon, "Watershed-base segmentation and region merging," *Computer Vision and Image Understanding* vol. 77, pp317-370, 2000.

Appendix

The sums of integrations in equation (10) first need be modified to discrete form:

$$F_1(C) + F_2(C) = \sum_{j=1}^{n_{int}-1}(u_j - \mu_{int0})^2 + \sum_{j=1}^{n_{ext}-1}(u_j - \mu_{ext0})^2 \quad \text{(A.1)}$$

where subscript "0" means the state before movement, and u_{int} and u_{ext} represent pixels inside and outside the water region respectively. After a single pixel flow, the numbers become n_{int}+1 and n_{ext}-1, respectively with corresponding changes in the statistics. By denoting the flooded pixel as u_n, we can deduce the changes. For the external term, the new term is

$$\begin{aligned}
F_2'(C) &= \sum_{j=1}^{n_{ext}-1}(u_j - \mu_{ext1})^2 \\
&= \sum_{j=1}^{n_{ext}-1}(u_j - \frac{\mu_{ext0} \times n_{ext} - u_n}{n_{ext}-1})^2 \\
&= \sum_{j=1}^{n_{ext}-1}(u_j - \frac{\mu_{ext0} \times (n_{ext}-1) + \mu_{ext0} - u_n}{n_{ext}-1})^2 \\
&= \sum_{j=1}^{n_{ext}-1}(u_j - \mu_{ext0} - \frac{\mu_{ext0} - u_n}{n_{ext}-1})^2 \\
&= \sum_{j=1}^{n_{ext}-1}(u_j - \mu_{ext0})^2 + (n_{ext}-1)(\frac{\mu_{ext0} - u_n}{n_{ext}-1})^2 + 2(\frac{u_n - \mu_{ext0}}{n_{ext}-1})\sum_{j=1}^{n_{ext}-1}(u_j - \mu_{ext0})
\end{aligned}$$

Denote $(u_n-\mu_{ext0})$ as Δ, then $\sum_{j=1}^{n_{ext}-1}(u_j - \mu_{ext0}) = -\Delta$(as $\sum_{j=1}^{n_{ext}}(u_j - \mu_{ext0}) = 0$), hence

$$\begin{aligned}
F_2'(C) &= \sum_{j=1}^{n_{ext}-1}(u_j - \mu_{ext0})^2 + \frac{\Delta^2}{n_{ext}-1} + 2\frac{\Delta}{n_{ext}-1}(-\Delta) \\
&= \sum_{j=1}^{n_{ext}}(u_j - \mu_{ext0})^2 - \Delta^2 - \Delta^2/(n_{ext}-1) \\
&= \sum_{j=1}^{n_{ext}}(u_j - \mu_{ext0})^2 - \Delta^2 n_{ext}/(n_{ext}-1)
\end{aligned}$$

The change to the external region is then $[-\Delta^2 n_{ext}/ (n_{ext}-1)]$. The coefficient is greater than 1, but for Δ, we have:

$$u_n - \mu_{ext0} = u_n - \frac{u_n + \sum_{j=1}^{n_{ext}-1}u_j}{n_{ext}} = \frac{n_{ext}-1}{n_{ext}}u_n - \frac{\sum_{j=1}^{n_{ext}-1}u_j}{n_{ext}}$$

So the maximum of Δ is achieved when u_n=1 (normalized) and u_j=0 for others. The external change should satisfy:

$$C_{ext} = \frac{n_{ext}-1}{n_{ext}}(u_n - \mu_{ext0})^2 \le \frac{n_{ext}}{n_{ext}-1}(\frac{n_{ext}-1}{n_{ext}})^2 = \frac{n_{ext}-1}{n_{ext}} < 1$$

Similarly, we can derive the change of the internal factor caused by the movement, which is given by

$$C_{int} = [n_{int}/(n_{int}+1)] \cdot (u_n - \mu_{int0})^2$$

The sum of the two changes gives equation (10). Since the absolute values of both terms fall in the range [0 1) for normalized images, the value range of the regional force is (-1 1), which can be directly applied to the formula